Very high cycle fatigue behavior of bridge steel welded joint

Chao He,[1, a)] Yongjie Liu,[1] Donghui Fang,[2] and Qingyuan Wang[1, b)]

[1)] *Department of Mechanics and Engineering Science, Sichuan University, Chengdu 610065, China*
[2)] *Department of Civil Engineering & Architecture, College of Jincheng, Sichuan University, Chengdu 610065, China*

Abstract Very high cycle fatigue (VHCF) behaviors of bridge steel (Q345) welded joints were investigated using an ultrasonic fatigue test system at room temperature with a stress ratio $R = -1$. The results show that the fatigue strength of welded joints is dropped by an average of 60% comparing to the base metal and the fatigue failure still occurred beyond 10^7 cycles. The fatigue fracture of welded joints in the low cycle regime generally occurred at the solder while at the heat-affected zone (HAZ) in the very high cycle regime. The fatigue fracture surface was analyzed with scanning electron microscopy (SEM), showing welding defects such as pore, micro-crack and inclusion were the main factors on decreasing the fatigue properties of welded joints. The effect of welding defects on the fatigue behaviors of welded joints was discussed in terms of experimental results and finite element simulations. © 2012 The Chinese Society of Theoretical and Applied Mechanics. [doi:10.1063/2.1203110]

Keywords welded joint, S–N curve, failure mechanism, very high cycle fatigue

In the applications of aircrafts, automobiles, off-shore structures and railway equipments, many components may experience nominal vibratory stress conditions over a long period of time, running up to several hundred million cycles.[1] In the practical application of welded structures, fatigue failure often occurs at the welded part, which may usually cause tremendous economic loss. From the investigation, it is found that the fatigue failure at the welded part sometimes occurs after the component experiences more than 10^8 stress cycles. Therefore, a deeply further study on fatigue behavior of welded joint, especially very high cycle fatigue behavior is a major concern in design and durability of welded engineering components and structures. Many materials, such as bearing steel, maraging steel and titanium alloy, have been investigated using ultrasonic fatigue test system for time saving because of its extremely high frequency of 20 kHz. It has been reported that the initiation sites of fatigue crack in low cycle regime and very high cycle regime were different.[2–4] While low cycle fatigue of steels usually involves fatigue crack initiation from inclusions/defects on the surface of the specimen, in the high cycle regime, the defects located within the specimen become favorable sites for crack initiation.[5] In the past twenty years, most of studies on fatigue were performed on base materials,[6–9] while fatigue behaviors of welded joints were rarely studied, especially very high cycle fatigue behaviors. In this paper, the ultrasonic fatigue testing technique was adopted to investigate the ultra-long life fatigue behaviors of Q345 welded joints.

The material used in the present study is a bridge steel (Q345). The chemical composition and mechanical properties are presented in Tables 1 and 2 respectively.

A shape of dog-bone is adopted to design specimens

Table 1. The chemical composition of Q345.

C	Si	Mn	S	P	Al
0.15	0.38	1.36	0.000 03	0.000 12	0.000 40

Table 2. Mechanical properties of Q345.

E /GPa	σ_s/MPa	σ_b/MPa	$\rho/(\mathrm{g \cdot cm^{-3}})$
201	420	570	7.85

and the dimensions are determined for the demands that the specimens have to resonate longitudinally with the ultrasonic fatigue testing system, based on analytical method. Geometrical characteristics of specimen are shown in Fig. 1.

Fatigue tests were performed on a piezoelectric fatigue machine (USF-2000, made in Japan) working on the principle of ultrasonic resonant loading. The standard resonance frequency of the system is 20 kHz, and details of the experimental setup for ultrasonic fatigue are described in the literature.[10] The tests were conducted in air at room temperature for different cyclic stresses based on the staircase method, under completely reversed cyclic loading conditions ($R = -1$) in ambient air at room temperature. During the test, specimens were cooled by a compressive condensing air cir-
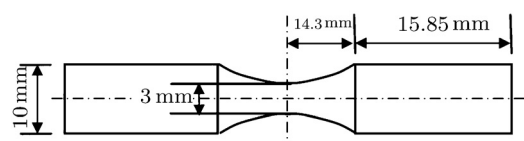

Fig. 1. Geometrical characteristics of specimens.

a)Email: hechaoscu@foxmail.com.
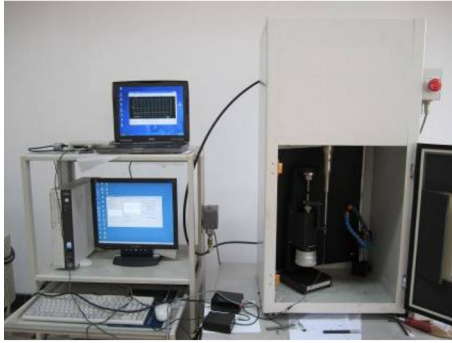b)Corresponding author. Email: wangqy@scu.edu.cn.
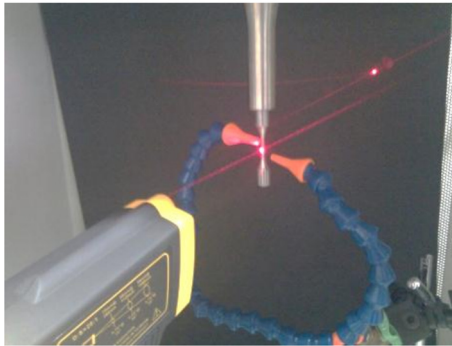
Fig. 2.   Ultrasonic fatigue test system.


Fig. 3.   Temperature test.

culation at 4°C to reduce the increase of temperature. The tests were controlled by a computer to guarantee the test system could automatically stop when the resonance was broken down due to the fatigue failure of the specimen. Moreover, an infrared thermometer was used to monitor variations of temperature on the surfaces of specimens during the test, as shown in Fig. 3.

Results from fatigue tests performed on base metal and welded joints are shown by means of the S–N data in Fig. 4. Generally, observations from the evolution of S–N data indicate that the fatigue life increases with the decrease of the applied maximum stress and there is no fatigue limit in the very high cycle regime. This conclusion are widely accepted by many researchers. Therefore, the limited fatigue life design method for engineering structures bearing very high cycle fatigue loads is not reliable. Comparing with the base metal, the fatigue resistance of welding joints is dropped by an average of 60% at the same fatigue life. The diamond in hollow indicates the specimen failed in the solder of welded joint. It can be seen that fatigue failure is prone to occur at the HAZ with high stress level in the low cycle fatigue regime. An explanation will be given in the following.

Fracture surfaces of failed specimens were investigated using SEM to capture the information on the fatigue crack initiation and propagation mechanisms involved, particularly at very high cycle. The SEM ob-
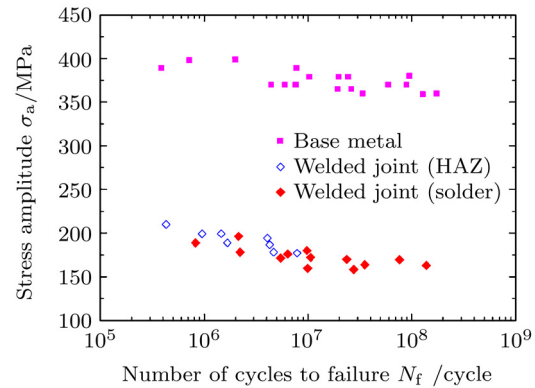
Fig. 4. S–N curves of Q345 specimens for base metal and welding joints.
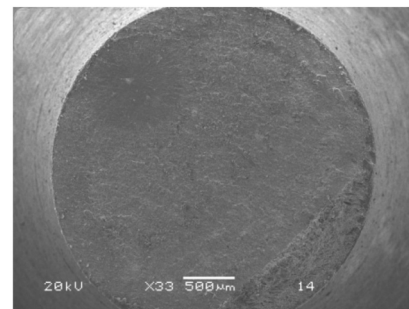
(a) Overall view of fracture surface
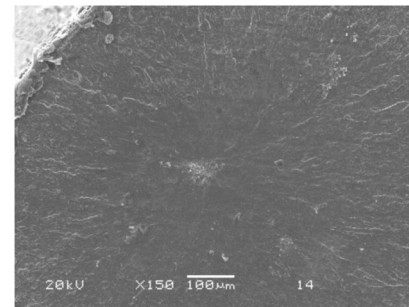
(b) Crack initiation area at high magnification (an inclusion)

Fig. 5.   Crack initiated from subsurface ($\sigma_a = 385$ MPa, $N_{\rm f} = 5.13 \times 10^7$ cycles).

servation shows the base metal has the following two crack initiation mechanisms: (1) The fatigue failure initiates mainly from the surface before 10^7 cycles; (2) The fatigue failure initiates basically from an internal inclusion beyond 10^7 cycles. Figure 5 shows a typical fatigue crack initiation from a subsurface inclusion for Q345 base metal in the very high cycle regime (over 10^7 cycles).

Differently, welded joints exhibit another two crack initiation and propagation mechanisms according to the location of fracture section in the specimens. On the

(a) Loose crystals

(b) Gas pore
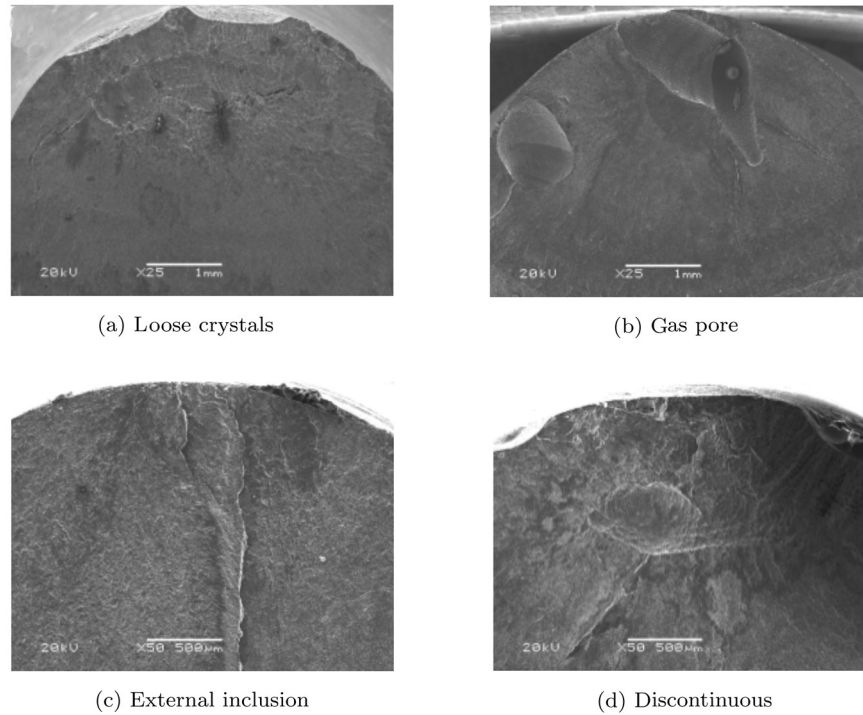

(c) External inclusion

(d) Discontinuous

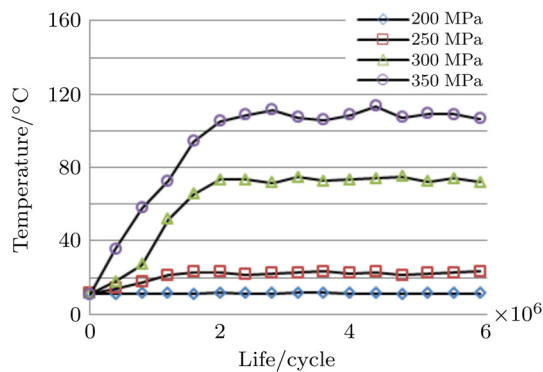Fig. 6.   The micrographs of the fracture surfaces of welded joints.

Fig. 7.   Temperature variations during the test.

one hand, fatigue fracture occurs in the HAZ or fusion zone. Interestingly, the crack initiation and propagation mechanisms in this case are very much similar to that of base metal, that is, crack initiates on the surface below 10^7 cycles and at an internal inclusion in the very high regime. On the other hand, fatigue failure appears in the weld zone. The analysis of fracture characteristic seems to be an extremely complicated work considering many internal defects caused by the welding process: lack of penetration, slag, gas pore, crack and overheating. Figure 6 shows the typical SEM micrographs of the fatigue crack initiating from different welding defects in the weld zone.

The effect of high frequency loading at 20 kHz on the fatigue life using ultrasonic fatigue testing should not be neglected. It is found that the temperature of the specimen subjected to cyclic deformation could rise due to the heat generated, and a greater increase of temperature at a higher frequency, especially at an ultrasonic frequency, is observed. In this test, temperatures at testing parts of the specimens were monitored by an infrared thermometer under different stress levels as shown in Fig. 7. It is found that the temperature rises slowly up to cycles, after that it almost retains at a horizontal level before the fatigue crack propagation starts. It is important to realize that the plastic zone around the crack tip could generate a large amount of heat, which causes a great increase of temperature before the specimen fracture. However, the process of crack propagation is very transient compared with the total fatigue life, therefore, the effect of temperature rising caused by high frequency in this test can be ignored.

Generally, according to the physical and chemical inhomogeneities, a welding joint can be divided into three parts: weld zone (WZ), fusion zone (FZ) and heat affected zone (HAZ). The surface hardness of a welded joint in the longitudinal direction is measured by Vickers. The results shows that the hardness of HAZ is the lowest, as shown in Fig. 8, which means the high plasticity at the HAZ. Hardness testing has always been an attractive way for scientists and industry to obtain valuable information on the material intrinsic mechanical properties and particularly the flow properties. A sim-
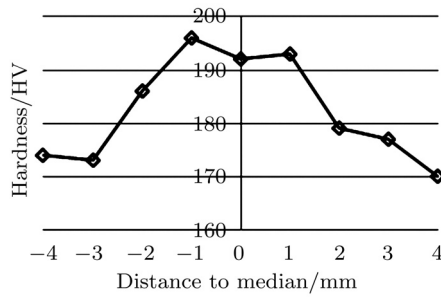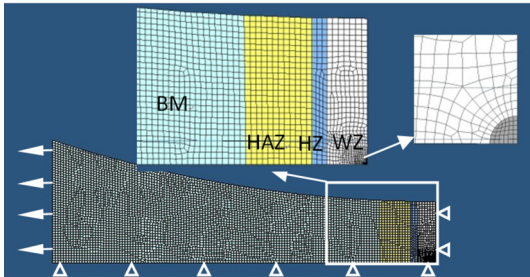
Fig. 8.   Surface hardness of a welded joint.

Fig. 9.   Finite element model of an inclusion in the specimen.

Fig. 10.   Maximum equivalent plastic strain around an inclusion at different positions.

ple linear relationship between the strength and hardness is proposed as follows[11–13]

$$H = c\sigma_y,$$

where H is the hardness value, c is the constant, and σ_y is the yield strength.

It is reported that local plastic area in the interior of material is the key factor to initiate a fatigue crack.[14] In order to figure out the effect of welding defect on the local plastic strain distribution at different locations (WZ, HZ and HAZ), a 2-D finite element model of the specimen is established with a tensile load of 400 MPa. A rigid inclusion with a diameter of 50 μm is embedded in the elasto-plastic matrix shown in Fig. 9. The Ramberg-Osgood constitutive model is adopted for the matrix with different yield strength at WZ (436 MPa), HZ (440 MPa), HAZ (404 MPa) and BM (420 MPa) in accordance with the hardness distribution in Fig. 8.

From the results shown in Fig. 10, it can be seen that the local plastic strain around the inclusion still existed even if the loading stress is lower than the yield stress. The maximum plastic stain in HAZ is the highest, which could explain why the fatigue failure is prone to occur at the HAZ under a high stress level. Moreover, the maximum plastic strain near the surface is higher than that within the specimen. This could also illuminate why fatigue cracks always initiate from surface in the low cycle regime.

Fatigue behaviors of base metal and welded joints of Q345 have been investigated using an ultrasonic fatigue test system. In order to study the effect of welding process on the 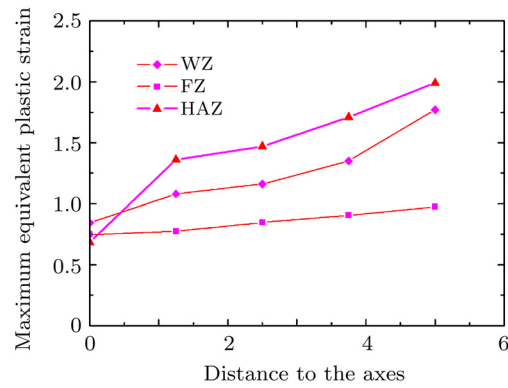fatigue strength, S–N curves of two groups of specimens are obtained and analyzed. The basic results of the investigation in this paper can be summarized as follows:

(1) The S–N curves of both the Q345 base metal and welded joints descend continuously during 10^5 and 10^9 cycles even if the cyclic load exceeds 10^7 cycles. Therefore, the very high cycle fatigue strength of welded structures serving under a gigacycle loading should be considered in the practical design.

(2) The fatigue strength of welded joints is dropped by an average of 60% comparing with the base metal in the long life range.

(3) By investigating the micrographs of the fractured surfaces, it is found that fatigue cracks for base metal usually initiate from surface defects below 10^7 cycles and from subsurface inclusions in the very high cycle regime. The fracture sections of welded joints are located at the WZ or HAZ. Finite element simulations shows that the HAZ is the weakest part in the welded joint under high stress level.

1. Q. Y. Wang, J. Y. Berard, and A. Dubarre, et al., Fatigue Fract. Engng. Mater. Struct. **22**, 667 (1999).
2. K. Shiozawa, L. Lu, and S. Ishihara, Fatigue Fract. Engng. Mater. Struct. **24**, 781 (2001).
3. Y. Ochi, T. Matsumura, and K. Masaki, et al., Fatigue Fract. Engng. Mater. Struct. **25**, 823 (2002).
4. S. Nishijima, and K. Kanazawa, Fatigue Fract. Engng. Mater. Struct. **22**, 601 (1999).
5. Q. Y. Wang, J. Y. Berard, and S. Rathery, et al., Fatigue Fract. Engng. Mater. Struct. **22**, 673 (1999).
6. D. H. Fang, Y. J. Liu, and Y. Y. Chen, et al., Science Paper Online. **7**, 480 (2009).
7. S. G. Chen, R. F. Liu, and Q. L. Ouyang, et al., Journal of Southwest University of Science and Technology **24**, 29 (2009).
8. Y. J. Liu, Q. L. Ouyang, and R. H. Tian et al., Journal of Medical Biomechanics **26**, 7 (2011).

9. X. J. Cao, Q. Y. Wang, and G. P. Chen, et al., Journal of Southwest University of Science and Technology **22**, 5 (2007).
10. B. Claude, Int. J. Fatigue **28**, 1438 (2006).
11. M. Zhou, J. S. Hu, and H. Zhang, Weld Res Suppl **78**, 305 (1999).
12. S. M. Zuniga, and S. D. Sheppard, Model Simul. Mater. Sci. Engng. **3**, 391 (1995).
13. G. F. V. Voort, Metallography Principles and Practice (ASM, USA, 1999).
14. G. C. Chai, N. Zhou, and S. Ciurea, et al., Scripta Materialia **66**, 769 (2012).